Letter

Chinese Science Bulletin

Geophysics

August 2011 Vol.56 No.23: 2419–2424
doi: 10.1007/s11434-011-4588-7

Far-field coseismic displacements associated with the 2011 Tohoku-oki earthquake in Japan observed by Global Positioning System

WANG Min[1*], LI Qiang[2], WANG Fan[1], ZHANG Rui[2], WANG YanZhao[1], SHI HongBo[2], ZHANG PeiZhen[1] & SHEN ZhengKang[3]

[1] *State Key Laboratory of Earthquake Dynamics, Institute of Geology, China Earthquake Administration, Beijing 100029, China;*
[2] *National Earthquake Infrastructure Service, China Earthquake Administration, Beijing 100036, China;*
[3] *Department of Geophysics, School of Earth and Space Science, Peking University, Beijing 100871, China*

Received April 6, 2011; accepted May 20, 2011

Analysis of GEONET observations covering the entire territory of Japan shows that the great Tohoku-oki earthquake that occurred on March 11, 2011 off the east coast of Honshu in Japan caused an eastward movement of the northern part of the island by as much as 5.3 m. The GPS data from TEONET in China were used to derive far-field coseismic displacements and to assess the impact of the Tohoku-oki earthquake on crustal deformation in eastern China. The results reveal that the coseismic horizontal displacements induced by the earthquake are the level of millimeters to centimeters in North and Northeast China, with a maximum of 35 mm. Strain analysis also indicates that the earthquake resulted in an increase in the tensile strain on the north-northeast trending faults in North and Northeast China. The tensile strain imposed on the Yilan-Yitong and Dunhua-Mishan faults is more significant than that imposed on the faults in North China; the maximum normal strain reaches about 40 nano-strain. Considering that the static Coulomb stress loaded on the faults is limited, its effect on the regional seismic activity may not be significant.

Tohoku-oki earthquake, far-field coseismic displacement, Tan-Lu fault zone, stress-strain, seismic activity

Citation: Wang M, Li Q, Wang F, et al. Far-field coseismic displacements associated with the 2011 Tohoku-oki earthquake in Japan observed by Global Positioning System. Chinese Sci Bull, 2011, 56: 2419–2424, doi: 10.1007/s11434-011-4588-7

On March 11, 2011, a huge M_w 9.0 earthquake occurred off the Pacific coast of northeastern Japan. The earthquake and the triggered tsunami caused massive destruction and huge numbers of casualties. According to the Japanese official statistics, as of April 4, the death toll exceeded 12000, more than 15000 people were reported missing, and the actual death toll was estimated to be over 27000. In northeastern Honshu, a large number of towns and villages located in the coastal area were swept out to the sea by the tsunami, and the four nuclear reactors of the Fukushima nuclear power plant were damaged and leaked radioactive contaminants into the air and water. The situation is still unfolding and it is difficult to evaluate its long-term effects.

*Corresponding author (email: mwang@gps.gov.cn)

The Japanese islands are located on the northwest rim of the Pacific Ocean, at the junction of the Pacific, North American, Philippine Sea and Eurasian plates. The earthquake occurred on the subduction zone between the Pacific and North American tectonic plates, in which the Pacific Plate moves westward at a rate of ~80 mm/a relative to the Eurasian Plate and eventually plunges underneath the North American Plate [1]. After the earthquake, many research institutions provided focal mechanism solutions, which all indicated that the earthquake occurred on the upper interface of the subducting slab, the rupture plane dipped to the west at an angle of 9°–14°, and the released seismic moment was about 3.6×10^{22} Nm, equivalent to a M_w 9.0 earthquake (Earthquake Research Institute, the University of Tokyo, http://www.eri.u-tokyo.ac.jp; United State Geological Survey (USGS), http://earthquake.usgs.gov; Harvard University,

http://www.seismology.harvard.edu), making it the fourth largest earthquake recorded by seismic instrumentation over the last century. The aftershock distribution showed that the rupture plane was ~100 km wide and extended ~350 km in a north-south direction along strike (USGS, http://earthquake.usgs.gov; Japanese Meteorological Agency, http://www.jma.go.jp/en/quake). Seismic waveform inversion has revealed that the rupture started at 38.1°N, 142.8°E and ~26 km deep, followed by a two-way rupture propagation with the largest slip of ~25 m, but dominated by thrust slip (http://www.geol.tsukuba.ac.jp/~yagi-y/EQ/Tohoku/index-e.html).

Since most of the earthquake rupture is located under the sea, detection of the rupture process relies on tele-recorded measurements. In addition to data from global and regional seismic networks, Global Positioning System (GPS) observations from Japan and its neighboring regions on the Asian continent are particularly important. After the earthquake, the ARIA team from JPL and Caltech made a rapid analysis of the data from GPS Earth Observation Network (GEO NET) and produced a coseismic displacement field for the Japanese islands (ftp://sideshow.jpl.nasa.gov/pub/usrs/ARIA/ARIA_coseismic_offsets.v0.3.table). The results show a considerable amount of eastward motion of northern Honshu and the horizontal displacement reached a maximum of ~5.3 m, with ~1.1 m of subsidence on the east coast. On the west coast of northern Honshu, ~0.7 m of horizontal displacement was found. The GPS displacement data were used to invert for the slip distribution of fault rupture and a maximum slip of ~21 m was obtained (http://earthquake.usgs.gov/earthquakes/world/japan/031111_M9.0prelim_geodetic_slip.php), which is comparable to the result obtained from seismic waveform inversion.

The coseismic displacement field obtained from the GPS stations in Japan provides information about near- and intermediate-field deformation. However, how is the far-field coseismic deformation distributed? What is the scope of its impact? Are the regions of Northeast and North China affected? If the coseismic effect exists, in what form does it appear? How does it impact the tectonic stress field in the Chinese continent? Answers to the above questions will not only help to understand the seismogenic structure and spatial distribution of slip for the Tohoku-oki earthquake, but also are essential in assessing the effect on the earthquake potential in North and Northeast China.

The national key infrastructure project "Tectonic and Environmental Observation Network in China" (hereinafter referred to as TEONET) provides important data for far-field seismic displacement monitoring. Construction of TEONET was completed in 2010 and primarily incorporates GPS technology to monitor crustal deformation. TEONET includes 260 continuous GPS stations, covering the entire Chinese continent, and its facilities are currently under trial operation. We have analyzed the GPS data from TEONET to derive the crustal deformation field in eastern China caused by the Tohoku-oki earthquake.

GAMIT software [2] was used to process the GPS data observed between March 8 and 13, 2011, from nearly 100 International Global Navigation Satellite System Service (IGS) stations and nearly 80 TEONET stations. Data recorded in an 18-h window on March 11 in the postseismic time period (06:00–24:00 UTC time) were used. For the IGS stations in Japan, the postseismic epoch was deduced using only the data observed on March 11, 06:00–24:00 UTC time. The GPS kinematic displacement results presented by the ARIA team showed continuous westward motion for the GEONET stations in the epicentral region after the quake, reaching a maximum of ~0.4 m at a coastal site during the period of 5:55–14:00 UTC time on March 11 (ftp://sideshow.jpl.nasa.gov/pub/usrs/ARIA/ARIA_postseismic_offsets.v0.3.table). Therefore, the displacements of IGS stations in Japan derived from 18-h data collected after the main shock must contain significant postseismic deformation signals. However, postseismic deformation in Japan should not have a significant impact on our analysis of far-field coseismic displacements. In addition, including the IGS stations in our processing helps establish a unified and self-consistent reference frame, providing assurance of a reliable result.

Figure 1 and Table 1 display the result of far-field coseismic displacements, from which it can be seen that the earthquake has induced significant coseismic horizontal displacements in Northeast China, North China, and the Korean Peninsula. A maximum displacement of ~35 mm in the south-southeast direction is observed near the triple border junction of China, Korea and Russia. The Korean Peninsula moved ~20 mm eastward. Displacements on the level of millimeters to centimeters in an east-west oriented direction are observed in the coastal area of North China; for example, 6–9 mm in Beijing and 8–9 mm in Tianjin respectively. Millimeter level displacements are detected in the coastal area of East China. The displacement field decays rapidly westward, and approaches zero in western China such as in Lanzhou, Chengdu and Kunming, and in northern Eurasia such as the region of Lake Baikal. The displacement vectors of IGS stations in Japan are similar to those given by the ARIA team. The overall deformation pattern agrees with that which was predicted by a thrust dislocation model in an elastic half-space [3]. The vertical coseismic displacements are too small to be detected.

Up to now, the coseismic slip distribution models of the Tohoku-oki earthquake have been all obtained from the inversion of seismic waveform data and/or GPS coseismic displacement data in Japan. Without constraints from far-field coseismic displacement data, how accurate would these models be? To answer this question, we used the far-field coseismic displacement data to test the slip distribution model by Wei et al. obtained from the inversion of GPS coseismic displacement and seismic waveform data (http://www.tectonics.caltech.edu/slip_history/2011_taiheiyo-oki/#slip). Forward prediction of Wei et al.'s model shows that

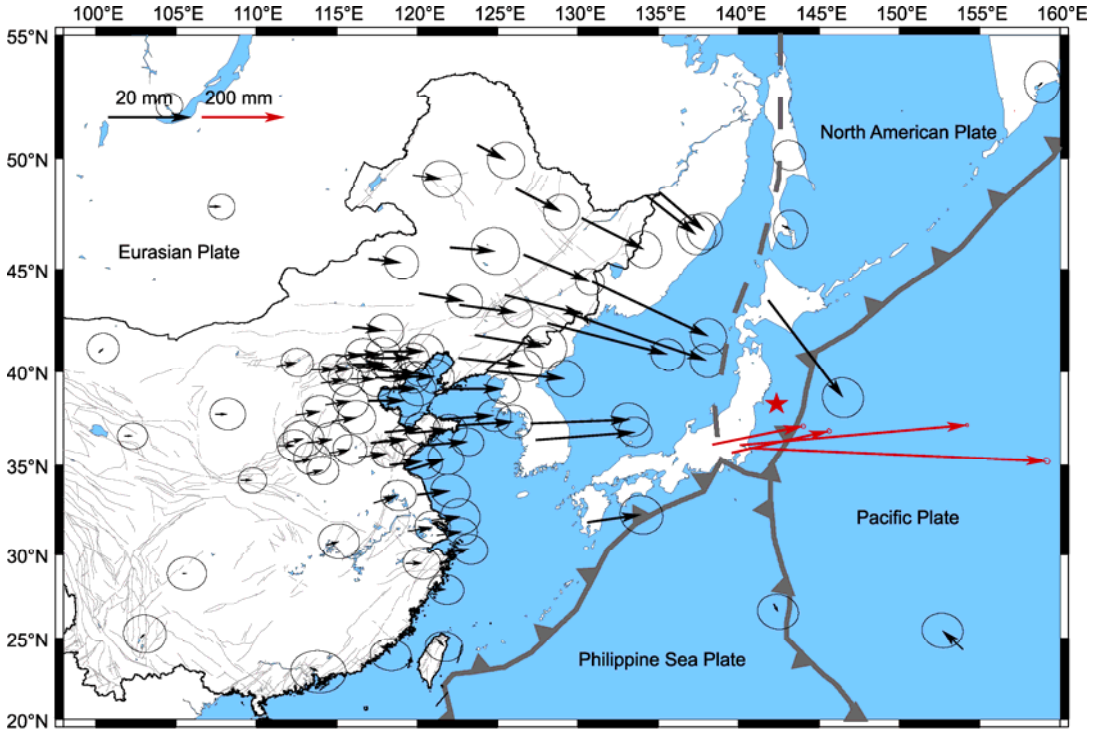

Figure 1 GPS-observed coseismic displacements in eastern China associated with the Tohoku-oki earthquake. The error ellipses represent 90% confidence.

systematic bias at the centimeter level exist between the observed and predicted data in the northeastern region of China, at the border between China and Russia, although the model fits most of the coseismic displacements in eastern China well. While the cause of the bias will be studied in the future, the far-field coseismic displacement data will provide help in refining the earthquake rupture model.

Whether or not the Tohoku-oki earthquake would affect local seismic activity in Northeast and North China is of particular concern. Ji (http://bbs.sciencenet.cn) proposed that the Tan-Lu fault zone in eastern China and the Japan-Izu-Bonin trench system belong to the same geological structure, and it is worth paying attention to the impact of the subduction of the Pacific Plate on the Tan-Lu fault zone. Previous studies considered that the westward subduction of the Pacific Plate caused deep-focused seismic activities in Northeast China, and further affected shallow seismic activities in Northeast and North China [4,5]. Li et al. [6] analyzed the seismicity pattern of $>M6$ events in North China and $>M7$ events in the arc-trench region off Japan, and found that the uneven distributions of the two groups of earthquakes over time have a certain pattern of synchronization. We therefore performed a brief analysis on the Tohoku-oki earthquake induced change in regional strain and possible seismic activity after the quake.

First, we derived the horizontal strain field by interpolating the GPS coseismic displacement field using the method of Shen et al. [7]. Figure 2 shows the horizontal principal strain components and reveals that the Tohoku-oki earthquake produced tensile strain on the north-northeast trending faults in North and Northeast China. The tensile strain imposed on the northern extensions of the Tan-Lu fault zone (also named as the Yilan-Yitong and Dunhua-Mishan faults) is relatively significant, with the maximum up to about 40 nano-strain. Assuming a shear modulus of 3.0×10^{10} Pa and the inner friction coefficient of 0.8 for the faults, and taking into account the change in the shear stress as well, we estimate that the maximum static Coulomb stress loaded by the coseismic deformation field would not exceed 0.002 MPa. The latest research showed that the Yilan-Yitong fault was tectonically active in Holocene and controlled the occurrence of small and moderate earthquake activities in Northeast China [8]. Therefore, the Tohoku-oki earthquake may have some minor effects on the seismic activity of the Yilan-Yitong fault, but little effect on other segments of the Tan-Lu fault zone and other faults in eastern China.

Our calculation also shows that Changbaishan volcano is located in a region of areal expansion caused by the Tohoku-oki earthquake (Figure 2). This means that the earthquake might cause the opening of the magma channel of the volcano and thus assist ascension of the magma flow [9]. Therefore, the earthquake could cause an increase in the activity of Changbaishan [10].

Second, we performed a statistical analysis on earthquake frequency from June 1, 2010 to March 31, 2011 in Northeast and North China (Figure 3). The results reveal that in these two regions, seismic activities do not increase significantly within three weeks after the earthquake, which

Table 1 GPS observed coseismic displacements associated with the Tohoku-oki earthquake

Station	Station location		Coseismic displacement		
	Longitude (°)	Latitude (°)	East (m)	North (m)	Correlation
AHBB	117.296	32.905	0.005 ± 0.0019	0.002 ± 0.0018	–0.043
BJFS	115.892	39.609	0.006 ± 0.0021	0.000 ± 0.0021	–0.042
BJGB	117.158	40.692	0.009 ± 0.0018	0.000 ± 0.0018	–0.048
BJSH	116.224	40.251	0.008 ± 0.0019	0.000 ± 0.0018	–0.044
BJYQ	115.968	40.370	0.008 ± 0.0018	0.000 ± 0.0017	–0.045
CHUN	125.444	43.790	0.018 ± 0.0018	–0.006 ± 0.0018	–0.057
DLHA	97.378	37.381	0.001 ± 0.0018	0.000 ± 0.0017	0.012
DXIN	100.201	40.984	0.001 ± 0.0018	0.001 ± 0.0018	0.002
GUAN	113.340	23.185	0.002 ± 0.0031	–0.001 ± 0.0025	–0.043
HAHB	114.519	35.658	0.005 ± 0.0019	0.001 ± 0.0018	–0.045
HAJY	112.447	35.163	0.004 ± 0.0021	0.001 ± 0.0019	–0.029
HECC	115.840	40.884	0.008 ± 0.0020	0.000 ± 0.0020	–0.051
HECD	117.918	41.016	0.010 ± 0.0021	0.000 ± 0.0020	–0.049
HECX	116.931	38.465	0.008 ± 0.0020	0.000 ± 0.0019	–0.052
HELQ	114.309	38.247	0.006 ± 0.0020	0.001 ± 0.0020	–0.042
HELY	114.707	37.399	0.006 ± 0.0021	0.001 ± 0.0020	–0.045
HETS	118.295	39.736	0.010 ± 0.0021	0.000 ± 0.0020	–0.053
HEYY	114.156	40.127	0.007 ± 0.0019	0.000 ± 0.0018	–0.046
HEZJ	114.900	40.828	0.007 ± 0.0021	0.000 ± 0.0020	–0.049
HLAR	119.741	49.270	0.006 ± 0.0022	–0.001 ± 0.0022	–0.108
HLFY	134.277	48.367	0.011 ± 0.0022	–0.010 ± 0.0024	–0.042
HLHG	130.236	47.353	0.015 ± 0.0020	–0.008 ± 0.0022	–0.045
HLWD	126.136	48.671	0.010 ± 0.0020	–0.005 ± 0.0021	–0.038
HRBN	126.620	45.703	0.015 ± 0.0016	–0.007 ± 0.0016	–0.045
JIXN	117.530	40.076	0.009 ± 0.0016	–0.001 ± 0.0015	–0.047
JLCB	128.106	42.411	0.029 ± 0.0019	–0.009 ± 0.0019	–0.060
JLYJ	129.505	42.875	0.033 ± 0.0019	–0.012 ± 0.0020	–0.058
JSLS	119.419	31.349	0.006 ± 0.0020	0.001 ± 0.0019	–0.049
JSLY	119.467	34.722	0.009 ± 0.0020	0.003 ± 0.0019	–0.066
JSNT	120.890	31.953	0.006 ± 0.0022	0.001 ± 0.0021	–0.056
JSYC	120.019	33.376	0.008 ± 0.0022	0.001 ± 0.0020	–0.056
KUNM	102.797	25.030	0.001 ± 0.0023	0.001 ± 0.0023	–0.035
LNDD	124.327	40.032	0.019 ± 0.0021	–0.002 ± 0.0021	–0.066
LNJZ	121.740	39.092	0.013 ± 0.0019	0.000 ± 0.0018	–0.055
LNSY	123.579	41.827	0.017 ± 0.0024	–0.003 ± 0.0024	–0.070
LNYK	122.603	40.684	0.015 ± 0.0019	–0.003 ± 0.0019	–0.055
LUZH	105.414	28.872	0.001 ± 0.0022	0.000 ± 0.0020	–0.008
NMAG	122.627	43.303	0.014 ± 0.0017	–0.003 ± 0.0017	–0.053
NMAL	120.113	43.863	0.011 ± 0.0020	–0.002 ± 0.0020	–0.056
NMDW	116.963	45.513	0.008 ± 0.0019	–0.001 ± 0.0019	–0.057
NMER	123.727	50.576	0.006 ± 0.0021	–0.003 ± 0.0022	–0.037
NMTK	111.252	40.261	0.005 ± 0.0018	0.001 ± 0.0017	–0.037
NMWL	122.027	46.041	0.011 ± 0.0027	–0.001 ± 0.0027	–0.060
NMZL	115.980	42.233	0.008 ± 0.0020	–0.001 ± 0.0020	–0.051
SDCY	119.460	36.754	0.010 ± 0.0019	0.001 ± 0.0018	–0.055
SDJX	116.351	35.427	0.007 ± 0.0018	0.001 ± 0.0017	–0.044
SDLY	118.288	35.000	0.008 ± 0.0022	0.001 ± 0.0021	–0.051
SDQD	120.304	36.077	0.011 ± 0.0018	0.000 ± 0.0017	–0.056

(*To be continued on the next page*)

(*Continued*)

Station	Station location		Coseismic displacement		
	Longitude (°)	Latitude (°)	East (m)	North (m)	Correlation
SDRC	122.421	37.170	0.014 ± 0.0020	0.001 ± 0.0019	–0.062
SDYT	121.436	37.483	0.013 ± 0.0019	0.001 ± 0.0018	–0.056
SDZB	117.992	36.806	0.009 ± 0.0020	0.001 ± 0.0019	–0.050
SHAO	121.200	31.100	0.006 ± 0.0017	0.001 ± 0.0015	–0.066
SUIY	130.908	44.433	0.028 ± 0.0020	–0.015 ± 0.0021	–0.062
SXCZ	113.180	36.225	0.005 ± 0.0021	0.001 ± 0.0020	–0.060
SXDT	113.392	40.122	0.006 ± 0.0019	0.000 ± 0.0018	–0.044
SXGX	111.900	36.252	0.004 ± 0.0023	0.001 ± 0.0022	–0.037
SXLF	111.371	36.084	0.004 ± 0.0020	0.001 ± 0.0019	–0.041
SXLQ	114.021	39.382	0.006 ± 0.0020	0.001 ± 0.0019	–0.055
SXTY	112.433	37.712	0.005 ± 0.0020	0.001 ± 0.0019	–0.041
TAIN	117.123	36.214	0.009 ± 0.0020	0.001 ± 0.0019	–0.049
TJBD	117.399	39.697	0.009 ± 0.0019	0.000 ± 0.0019	–0.050
TJBH	117.689	39.084	0.009 ± 0.0021	0.000 ± 0.0020	–0.051
WUHN	114.357	30.532	0.003 ± 0.0023	0.001 ± 0.0020	–0.043
XIAA	108.986	34.178	0.003 ± 0.0016	0.000 ± 0.0015	–0.017
XIAM	118.083	24.450	0.001 ± 0.0023	–0.001 ± 0.0019	–0.058
XNIN	101.774	36.601	0.001 ± 0.0017	0.000 ± 0.0016	0.002
YANC	107.437	37.779	0.003 ± 0.0020	0.000 ± 0.0019	–0.018
ZHNZ	113.105	34.521	0.004 ± 0.0018	0.001 ± 0.0017	–0.035
ZJJD	119.274	29.475	0.004 ± 0.0020	0.000 ± 0.0018	–0.056
ZJWZ	120.763	27.934	0.004 ± 0.0019	0.000 ± 0.0017	–0.065
ZJZS	121.989	30.071	0.005 ± 0.0019	0.001 ± 0.0018	–0.068
AIRA	130.600	31.824	0.013 ± 0.0024	0.002 ± 0.0022	–0.068
CCJ2	142.195	27.068	0.001 ± 0.0022	–0.002 ± 0.0021	–0.079
CNMR	145.743	15.230	0.001 ± 0.0029	0.000 ± 0.0027	–0.015
DAEJ	127.374	36.399	0.023 ± 0.0019	0.002 ± 0.0018	–0.064
GUAM	144.868	13.589	0.001 ± 0.0030	0.001 ± 0.0029	–0.175
IRKT	104.316	52.219	0.001 ± 0.0015	0.000 ± 0.0015	0.012
KGNI*	139.488	35.710	0.239 ± 0.0030	0.058 ± 0.0035	–0.163
KHAJ	135.046	48.521	0.011 ± 0.0020	–0.011 ± 0.0021	–0.034
KSMV*	140.658	35.955	0.716 ± 0.0028	–0.035 ± 0.0032	–0.186
MCIL	153.979	24.290	-0.006 ± 0.0023	0.006 ± 0.0021	–0.055
MTKA*	139.561	35.680	0.236 ± 0.0025	0.057 ± 0.0025	–0.099
PETS	158.650	53.023	0.001 ± 0.0020	0.001 ± 0.0025	0.013
STK2	141.845	43.529	0.017 ± 0.0023	–0.025 ± 0.0024	–0.041
SUWN	127.054	37.276	0.024 ± 0.0020	0.001 ± 0.0019	–0.099
TSKB*	140.087	36.106	0.547 ± 0.0020	0.051 ± 0.0020	–0.103
TWTF	121.165	24.954	0.003 ± 0.0021	–0.002 ± 0.0017	–0.064
ULAB	107.052	47.865	0.003 ± 0.0015	0.000 ± 0.0015	0.004
USUD*	138.362	36.133	0.219 ± 0.0024	0.048 ± 0.0024	–0.102
YSSK	142.717	47.030	0.002 ± 0.0019	–0.001 ± 0.0023	–0.053

* represents the IGS station in Japan, whose coseismic displacements were derived from 18-h data after the main shock.

is different from increased seismic activities we observed in the Sichuan-Yunnan region after the 2004 Sumatra earthquake [11]. This also suggests that the effects of the Tohoku-oki earthquake on faults in Northeast and North China are limited.

It is worth mentioning that large earthquakes affect regional stress-strain field. This effect can last for years, decades, or even centuries as the results of afterslip on the fault plane and viscoelastic relaxation in the lower crust and upper mantle. Previous studies have shown that in some

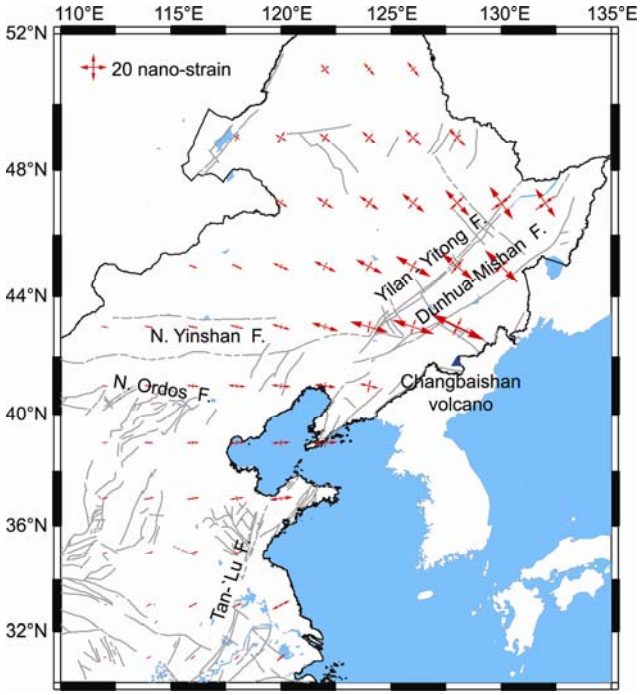

Figure 2 Horizontal principal strain components caused by the Tohoku-oki earthquake.

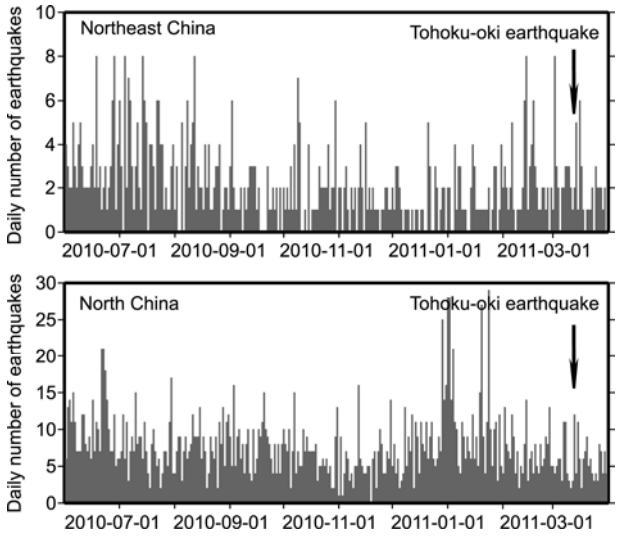

Figure 3 Frequencies of earthquakes in Northeast and North China before and after the Tohoku-oki earthquake.

cases the seismic moment released by afterslip following large interplate earthquakes could even be comparable to that released by the coseismic rupture [12–14]. Thus viscoelastic relaxation in the lower crust and upper mantle could affect much wider regions. Therefore, to further understand tectonic loading processes and associated changes of earthquake potentials, in the next few years we need to monitor the temporal evolution of the stress-strain field caused by the Tohoku-oki earthquake by analyzing GPS data from TEONET. At the same time, it will be necessary to continue studying the triggering effect of the Tohoku-oki earthquake on the Changbaishan volcano, and closely monitor volcanic activity in the region to provide a basis for earthquake disaster mitigation in Northeast and North China.

After the Tohoku-oki earthquake, GPS observations from TEONET allowed us to immediately assess the change in crustal movement caused by the earthquake. Also, the observations make up an important and fundamental dataset for understanding earthquake rupture processes. Compared with GPS observations from episodic campaign surveys, continuous GPS observations are more efficient and more accurate for capturing coseismic and postseismic deformation fields and their temporal evolution. The completion and operation of TEONET enhances abilities to monitor crustal deformation, capture earthquake precursors, and gain insights into the entire spatiotemporal deformation field associated with tectonic and seismogenic processes.

The authors gratefully acknowledge the suggestions of anonymous reviewers that helped in improving the quality of the paper. This work was supported by the State Key Laboratory of Earthquake Dynamics (LED2009A02) and the National Key Infrastructure Project "Tectonic and Environmental Observation Network in China".

1 DeMets C, Gordon R G, Argus D F, et al. Geophys Res Lett, 1994, 21: 2191–2194
2 Herring T A, King R W, McClusky S C. GAMIT reference manual: GPS Analysis at MIT. Release 10.4. Department of Earth, Atmospheric, and Planetary Sciences, Massachusset Institute of Technology, Cambridge MA, 2010
3 Okada Y. Bull Seism Soc Am, 1985, 75: 1135–1154
4 Sun W B, He Y S, Li Y B. Acta Seismol Sin, 1985, 7: 33–44
5 Meng X S, Zheng H, Jiang J H. Seismol Res Northeast Chin, 2003, 19: 13–18
6 Li W Y, Wang X Y. Earthquake, 1996, 16: 219–224
7 Shen Z-K, Jackson D D, Ge B X. J Geophys Res, 1996, 101: 27957–27980
8 Min W, Jiao D C, Zhou B G, et al. Seismol Geol, 2011, 33: 141–150
9 Walter T R, Amelung F. Geology, 2007, 35: 539–542
10 Wang F, Shen Z K, Wang Y Z, et al. Chinese Sci Bull, 2011, 56: 2077–2081
11 Wang M, Zhang P Z, Shen Z K, et al. Chinese Sci Bull, 2006, 51: 1771–1775
12 Heki K, Miyazaki S, Tsuji H. Nature, 1997, 386: 595–598
13 Nishimura T, Miura S, Tachibana K, et a1. Tectonophysics, 2000, 323: 217–238
14 Ozawa S, Kaidzu M, Murakami M, et a1. Earth Planets Space, 2004, 56: 675–680